

## Electronic Supplementary Information

### New Ternary Ligands Consisting of a N4 Bridging Ligand and Two Terpyridines, and Their Co(II) and Ni(II) Dinuclear Complexes. Structure, Redox Properties, and Reaction with Acid.

Hiroki Kon and Toshi Nagata

Experimental procedures for synthesis of the compounds **5**, **6b**, **7b**, **8b** and **2**.

Figure S-1. Drawings of the X-ray structure of the complex cation  $[(\mathbf{1})\text{Ni}_2(\mu\text{-Cl})]^{3+}$ ; (a) an ORTEP side view, (b) bottom view, (c) space-filling model. The dotted arrows in (c) indicate the 3-hydrogens causing steric repulsion with the phthalazine *peri* hydrogens.

Figure S-2. Partial structures of N4 bridge and metal ions in (a)  $[(\mathbf{1})\text{Co}_2(\mu\text{-OH})]^{3+}$ , (b)  $[(\mathbf{1})\text{Ni}_2(\mu\text{-Cl})]^{3+}$ .

Figure S-3. Constant potential bulk electrolysis with coulometry for (a)  $[(\mathbf{1})\text{Co}_2(\mu\text{-OH})](\text{PF}_6)_3$ , (b)  $[(\mathbf{1})\text{Ni}_2(\mu\text{-Cl})](\text{PF}_6)_3$ . Solvent: DMF with 0.1 M  $\text{Bu}_4\text{NClO}_4$ , glassy carbon electrode.

Figure S-4. Changes of the UV-visible absorption spectra upon electrochemical reduction. (a) ligand **1**, (b)  $[(\mathbf{1})\text{Co}_2(\mu\text{-OH})](\text{PF}_6)_3$ , (c)  $[(\mathbf{1})\text{Ni}_2(\mu\text{-Cl})](\text{PF}_6)_3$ . Solvent: DMF with 0.1 M  $\text{Bu}_4\text{NClO}_4$ .

Figure S-5. Scan rate dependence of the cyclic voltammograms of (a)  $[(\mathbf{1})\text{Co}_2(\mu\text{-OH})]^{3+}$  and (b)  $[(\mathbf{1})\text{Ni}_2(\mu\text{-Cl})]^{3+}$ , in DMF with 0.1 M  $\text{Bu}_4\text{NPF}_6$ .

Figure S-6. Cyclic voltammograms (positive side) for (a)  $[(\mathbf{1})\text{Co}_2(\mu\text{-OH})]^{3+}$ , (b)  $[(\mathbf{1})\text{Ni}_2(\mu\text{-Cl})]^{3+}$ , (c)  $[(\mathbf{2})\text{Co}_2(\mu\text{-OH})]^{3+}$  (d) cobalt(II) mononuclear complex and (e) nickel(II) mononuclear complex in  $\text{CH}_3\text{CN}$  with 0.1 M  $\text{Bu}_4\text{NPF}_6$ .

Figure S-7. ESI-MS spectra of (a)  $[(\mathbf{1})\text{Co}_2(\mu\text{-OH})]^{3+}$ , (b) after the addition of 10 eq.  $\text{CF}_3\text{SO}_3\text{H}$  and (c) after the addition of 30 eq.  $\text{CF}_3\text{SO}_3\text{H}$  in  $\text{CH}_3\text{CN}$ .

Figure S-8. CVs of (a)  $[(\mathbf{2})\text{Co}_2(\mu\text{-OH})]^{3+}$  and (b)  $[(\mathbf{1})\text{Ni}_2(\mu\text{-Cl})]^{3+}$ , with the addition of  $\text{CF}_3\text{SO}_3\text{H}$ .

Table S-1. Selected bond distances (Å) and angles (deg) for  $[(\mathbf{1})\text{Ni}_2(\mu\text{-Cl})]^{3+}$ .

### Synthetic procedures for the compound **5**, **6b**, **7b**, **8b** and **2**.

The compound **4** was synthesized according to the literature procedure.<sup>11</sup>

**2-Bromo-5-(1,3-dioxan-2-yl)pyridine.** 6-Bromo-3-pyridinecarbaldehyde (**4**, 889.0 mg, 4.78 mmol), 1,3-propanediol (1.46 g, 19.2 mmol), *p*-toluenesulfonic acid (278.0 mg, 1.46 mmol) were dissolved in CH<sub>2</sub>Cl<sub>2</sub> (10 ml), and stirred at room temperature. After 12 hr, the reaction mixture was washed with sat. NaHCO<sub>3</sub> aq. and the organic phase was dried over Na<sub>2</sub>SO<sub>4</sub>, and evaporated. Yield: 1.09 g (4.48 mmol, 94% as white crystalline powder). <sup>1</sup>H NMR (400 MHz, CDCl<sub>3</sub>, 25 °C, TMS): δ = 8.44 (d, <sup>4</sup>*J*(H,H) = 2.4 Hz, 1H; Ar-6-H), 7.66 (dd, <sup>3</sup>*J*(H,H) = 8.4 Hz, <sup>4</sup>*J*(H,H) = 2.4 Hz, 1H; Ar-4-H), 7.47 (d, <sup>3</sup>*J*(H,H) = 8.4 Hz, 1H; Ar-3-H), 5.51 (s, 1H; dioxane-2-H), 4.24-4.29 (m, 2H; dioxane-4,6-H), 3.94-4.01 (m, 2H; dioxane-4,6-H), 2.15-2.28 (m, 1H; dioxane-5-H), 1.44-1.50 ppm (m, 1H; dioxane-5-H).

**5-(1,3-Dioxan-2-yl)-2-tributylstannylpyridine (**5**).** 2-Bromo-5-(1,3-dioxan-2-yl)pyridine (2.1 g, 8.61 mmol) was dissolved in dry Et<sub>2</sub>O (80 ml) and kept under Ar. The solution was cooled to -80 °C and *n*-BuLi (1.6 M in hexane, 6.5 ml, 10.4 mmol) was added slowly using a dropping funnel. After stirring for 90 min at -80 °C under Ar, Bu<sub>3</sub>SnCl (3.1 ml, 11.4 mmol) was added to the solution. The reaction mixture was stirred for 120 min at -80 °C under Ar, and allowed to warm up to room temperature overnight. After the reaction, the solution was filtered from inorganic salts and the residue was washed with small amount of diethyl ether. The filtrate was evaporated and dried in vacuo to obtain the yellow-orange oil. Finally, the product was purified by column chromatography (alumina, hexane/CH<sub>2</sub>Cl<sub>2</sub> = 100/0 ~ 70/30). Yield: 2.5 g (5.51 mmol, 64% as pale yellow oil). <sup>1</sup>H NMR (400 MHz, CDCl<sub>3</sub>, 25 °C, TMS): δ = 8.80 (d, <sup>4</sup>*J*(H,H) = 1.0 Hz, 1H; Ar-6-H), 7.62 (dd, <sup>3</sup>*J*(H,H) = 8.0 Hz, <sup>4</sup>*J*(H,H) = 2.4 Hz, 1H; Ar-4-H), 7.41 (d, <sup>3</sup>*J*(H,H) = 8.4 Hz, 1H; Ar-3-H), 5.51 (s, 1H; dioxane-2-H), 4.24-4.29 (m, 2H; dioxane-4,6-H), 3.96-4.02 (m, 2H; dioxane-4,6-H), 2.17-2.28 (m, 1H; dioxane-5-H), 0.84-1.60 ppm (m, 28H; dioxane-5-H, Bu<sub>3</sub>Sn-).

**3,6-Bis[5-(1,3-dioxane-2-yl)-2-pyridyl]pyridazine (**6b**).** This compound was prepared by same procedure of **6a** using **5** (416 mg, 0.92 mmol), 3,6-dichloropyridazine (60.2 mg, 0.40 mmol), Pd(PPh<sub>3</sub>)<sub>4</sub> (15.2 mg, 0.013 mmol), CuI (5.1 mg, 0.027 mmol) and DMF (2 ml). Yield: 122 mg (0.30 mmol, 74%). <sup>1</sup>H NMR (400 MHz, CDCl<sub>3</sub>, 25 °C, TMS): δ = 8.81 (s, 2H; py-6-H), 8.75 (d, <sup>3</sup>*J*(H,H) = 8.0 Hz, 2H; py-3-H), 8.68 (s, 2H; pyridazine-4,5-H), 8.02 (dd, <sup>3</sup>*J*(H,H) = 8.0 Hz, <sup>4</sup>*J*(H,H) = 2.0 Hz, 2H; py-4-H), 5.65 (s, 2H; dioxane-2-H), 4.30-4.34 (m, 4H; dioxane-4,6-H), 4.01-4.08 (m, 4H; dioxane-4,6-H), 2.22-2.32 ppm (m, 2H; dioxane-5-H).

**2,2'-(3,6-Pyridazinediyl)dipyridine-5,5'-dicarbaldehyde (**7b**).** This compound was prepared by same procedure of **7a** using **6b** (115 mg, 0.283 mmol). Yield: 78.4 mg (0.270 mmol, 95%). <sup>1</sup>H NMR (400 MHz, CDCl<sub>3</sub>, 25 °C, TMS): δ = 10.23 (s, 2H; -CHO), 9.21 (d, <sup>4</sup>*J*(H,H) = 2.2 Hz,

2H; py-2-H), 8.97 (d,  $^3J(\text{H,H}) = 8.0$  Hz, 2H; py-5-H), 8.83 (s, 2H; pyridazine-4,5-H), 8.39 (dd,  $^3J(\text{H,H}) = 8.0$  Hz,  $^4J(\text{H,H}) = 2.2$  Hz, 2H; py-4-H).

**2,2'-(3,6-Pyridazinediyl)dipyridine-5,5'-dicarboxylic acid (8b).** This compound was prepared by same procedure of **8a** using **7b** (74.2 mg, 0.255 mmol), NaClO<sub>2</sub> (80%, 86.4 mg, 0.768 mmol) and NaH<sub>2</sub>PO<sub>4</sub>•H<sub>2</sub>O (106 mg, 0.682 mmol). Yield: 66.9 mg (0.207 mmol, 81%). This compound was used to next reaction without further purification.

**Compound 2.** This compound was prepared by same procedure of **1** using **8b** (66.9 mg, 0.207 mmol), **9** (212 mg, 0.533 mmol), DMAP (122 mg, 0.998 mmol), HOBT•H<sub>2</sub>O (143 mg, 1.06 mmol) and EDC•HCl (194 mg, 1.02 mmol). Yield: 161 mg (0.149 mmol, 72%). Elemental analysis calcd (%) for **2**•0.5H<sub>2</sub>O (C<sub>66</sub>H<sub>55</sub>N<sub>12</sub>O<sub>4.5</sub>) C 72.85, H 5.09, N 15.45; found: C 72.86, H 4.99, N 15.36. <sup>1</sup>H NMR (400 MHz, CDCl<sub>3</sub>, 25 °C, TMS): δ = 8.82 (d,  $^4J(\text{H,H}) = 2.0$  Hz, 2H; py-2-H), 8.68 (m, 4H; trpy-3'-H, trpy-5'-H), 8.55-8.63 (m, 10H; trpy-3-H, trpy-6-H, trpy-3''-H, trpy-6''-H, py-5-H), 8.51 (s, 2H; pyridazine-4,5-H), 7.78-7.84 (6H; py-4-H, trpy-4-H, trpy-4''-H), 7.54 (dd,  $^3J(\text{H,H}) = 7.6$  Hz,  $^4J(\text{H,H}) = 1.6$  Hz, 2H; Ar-6-H), 7.40 (td,  $^3J(\text{H,H}) = 8.0$  Hz,  $^4J(\text{H,H}) = 1.6$  Hz, 2H; Ar-5-H), 7.26 (overlapping with CHCl<sub>3</sub>, 4H; trpy-5,5'), 7.00-7.10 (m, 4H; Ar-3-H, Ar-4-H), 6.86 (t,  $^3J(\text{H,H}) = 5.6$  Hz, 2H; amide-H), 4.16 (t,  $^3J(\text{H,H}) = 4.4$  Hz, 4H; -NHCH<sub>2</sub>CH<sub>2</sub>CH<sub>2</sub>CH<sub>2</sub>O-), 3.51 (q,  $^3J(\text{H,H}) = 6.0$  Hz, 4H; -NHCH<sub>2</sub>CH<sub>2</sub>CH<sub>2</sub>CH<sub>2</sub>O-), 1.90-1.96 ppm (m, 8H; -NHCH<sub>2</sub>CH<sub>2</sub>CH<sub>2</sub>CH<sub>2</sub>O-). <sup>13</sup>C NMR (100 MHz, CDCl<sub>3</sub>, 25 °C, TMS): δ = 165.6 (-NHCO-), 157.7 (Ar-2-C), 156.5 (trpy-2'-C, trpy-6'-C), 156.0 (trpy-2-C, trpy-2''-C), 155.2 (py-2-C), 155.0 (py-6-C), 149.0 (trpy-6-C, trpy-6''-C), 148.6 (Pyd-3,6-C), 148.2 (trpy-4'-C), 137.1 (trpy-4-C, trpy-4''-C), 135.5 (Py-4-C), 131.1 (py-3-C), 130.9 (Ar-4-C), 130.3 (Ar-6-C), 128.3 (Ar-1-C), 125.5 (py-5-C), 123.9 (trpy-5-C, trpy-5''-C), 122.0 (trpy-3-C, trpy-3''-C), 121.6 (trpy-3'-C, trpy-5'-C), 121.2 (Pyd-4,5-C), 121.0 (Ar-5-C), 112.3 (Ar-3-C), 67.8 (-NHCH<sub>2</sub>CH<sub>2</sub>CH<sub>2</sub>CH<sub>2</sub>O-), 39.7 (-NHCH<sub>2</sub>CH<sub>2</sub>CH<sub>2</sub>CH<sub>2</sub>O-), 26.7 (-NHCH<sub>2</sub>CH<sub>2</sub>CH<sub>2</sub>CH<sub>2</sub>O-), 26.4 ppm (-NHCH<sub>2</sub>CH<sub>2</sub>CH<sub>2</sub>CH<sub>2</sub>O-).

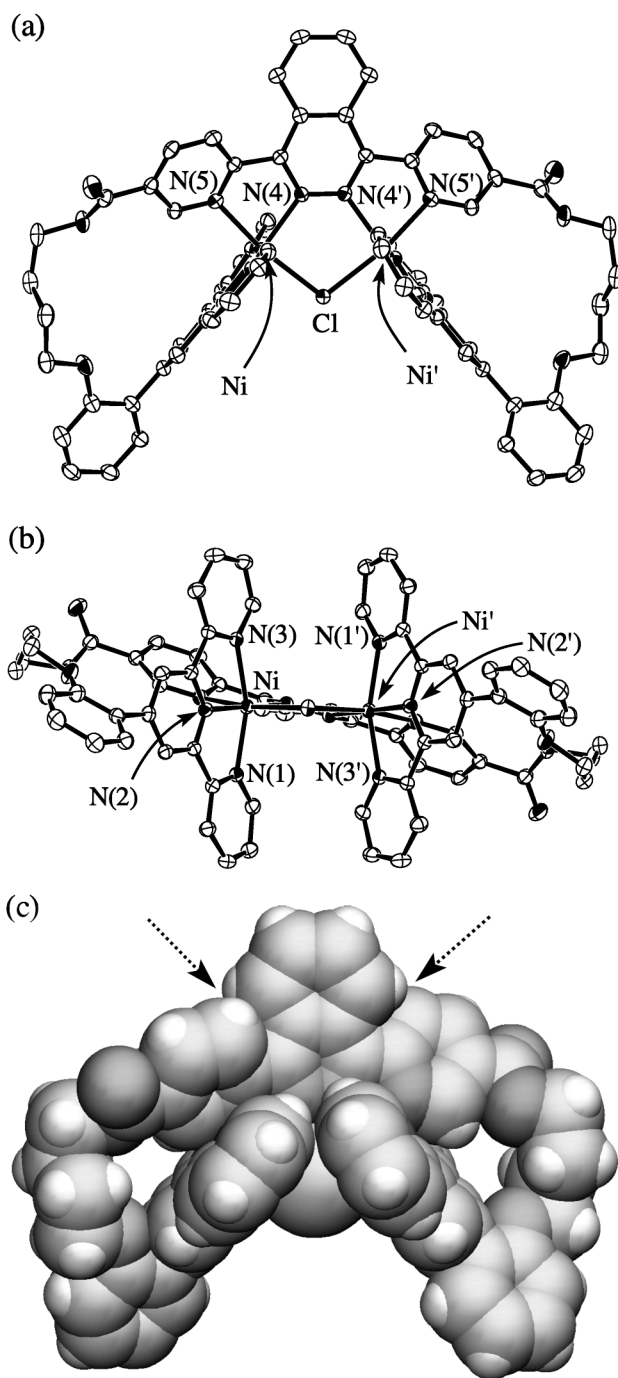


Figure S-1. Drawings of the X-ray structure of the complex cation  $[(1)Ni_2(\mu-Cl)]^{3+}$ ; (a) an ORTEP side view, (b) bottom view, (c) space-filling model. The dotted arrows in (c) indicate the 3-hydrogens causing steric repulsion with the phthalazine *peri* hydrogens.

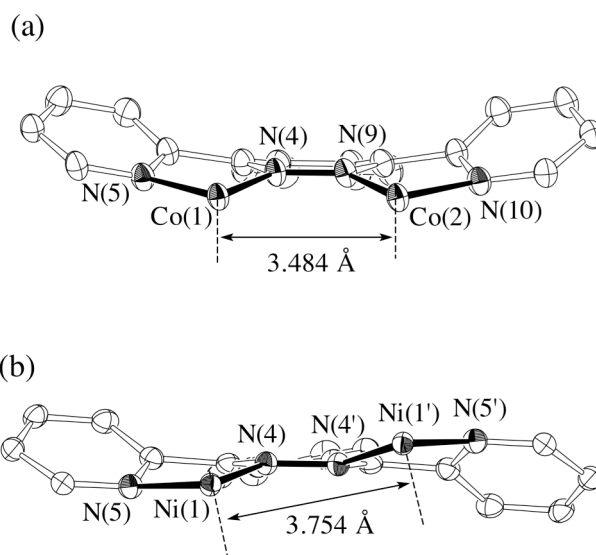


Figure S-2. Partial structures of N4 bridge and metal ions in (a)  $[(1)\text{Co}_2(\mu\text{-OH})]^{3+}$ , (b)  $[(1)\text{Ni}_2(\mu\text{-Cl})]^{3+}$ .

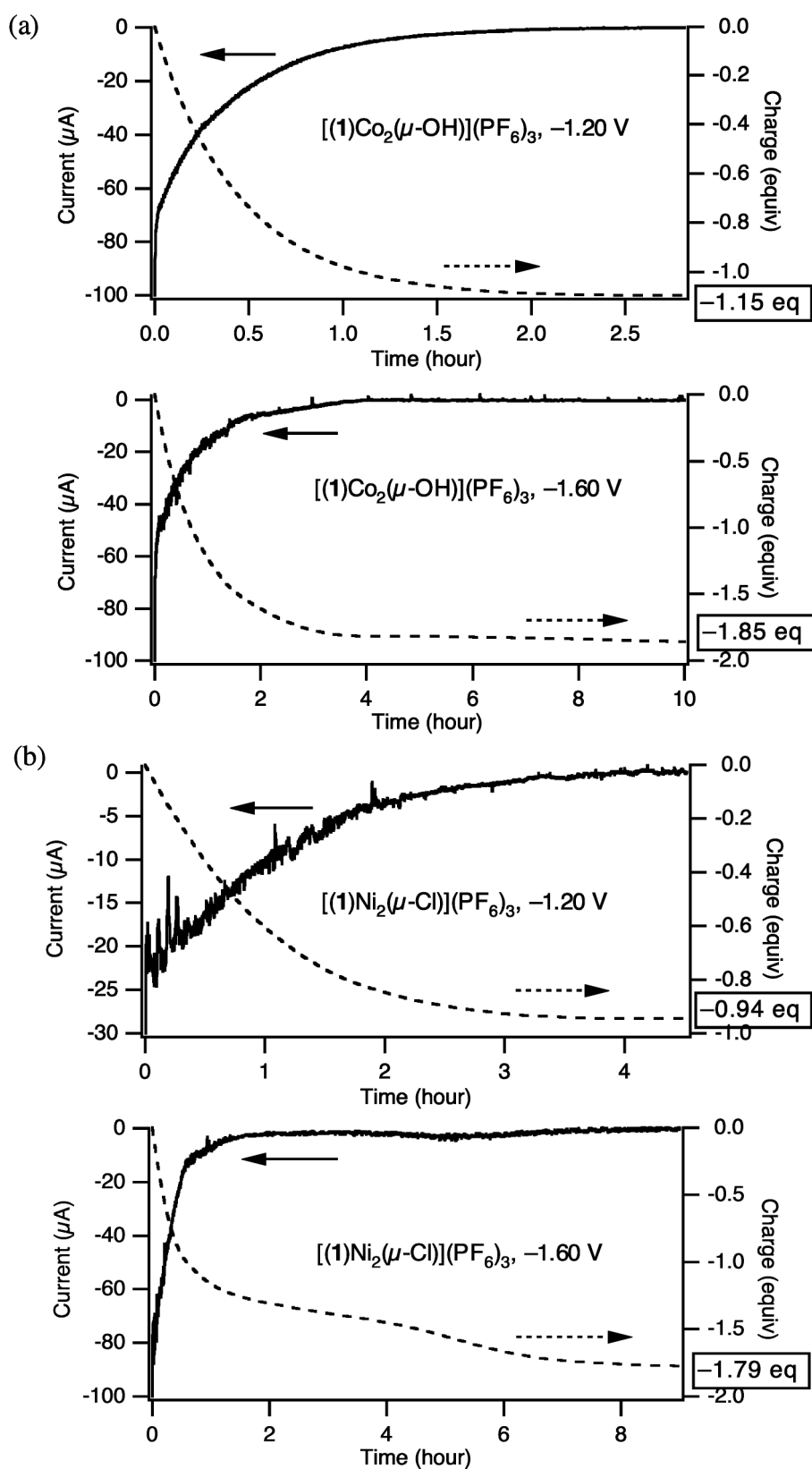


Figure S-3. Constant potential bulk electrolysis with coulometry for (a)  $[(1)Co_2(\mu-OH)](PF_6)_3$ , (b)  $[(1)Ni_2(\mu-Cl)](PF_6)_3$ . Sample concentration 0.50 mM in DMF with 0.1 M  $Bu_4NClO_4$ , glassy carbon electrode. The potentials of the working electrode are given in reference to  $Fc/Fc^+$ .

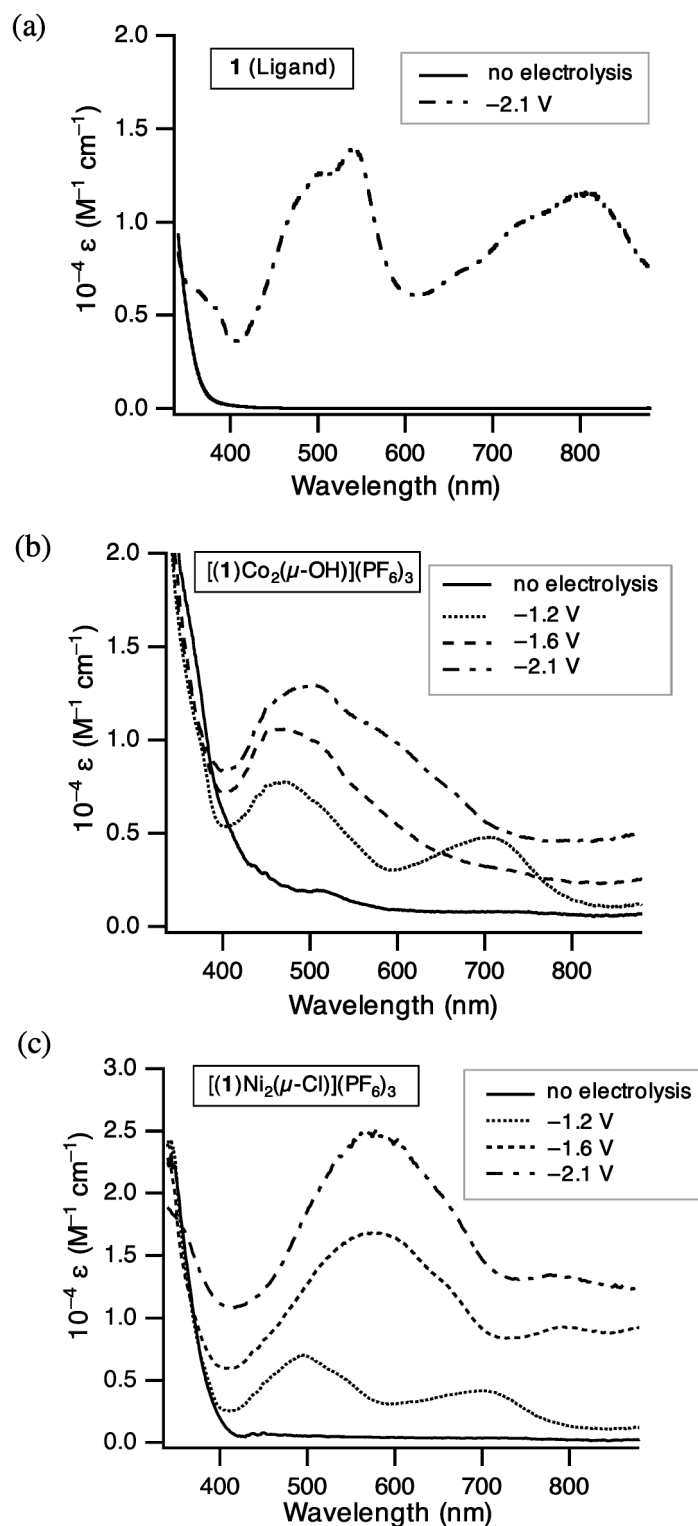


Figure S-4. Changes of the UV-visible absorption spectra upon electrochemical reduction. (a) ligand **1**, (b)  $[(1)Co_2(\mu-OH)](PF_6)_3$ , (c)  $[(1)Ni_2(\mu-Cl)](PF_6)_3$ . Solvent: DMF with 0.1 M  $Bu_4NClO_4$ .

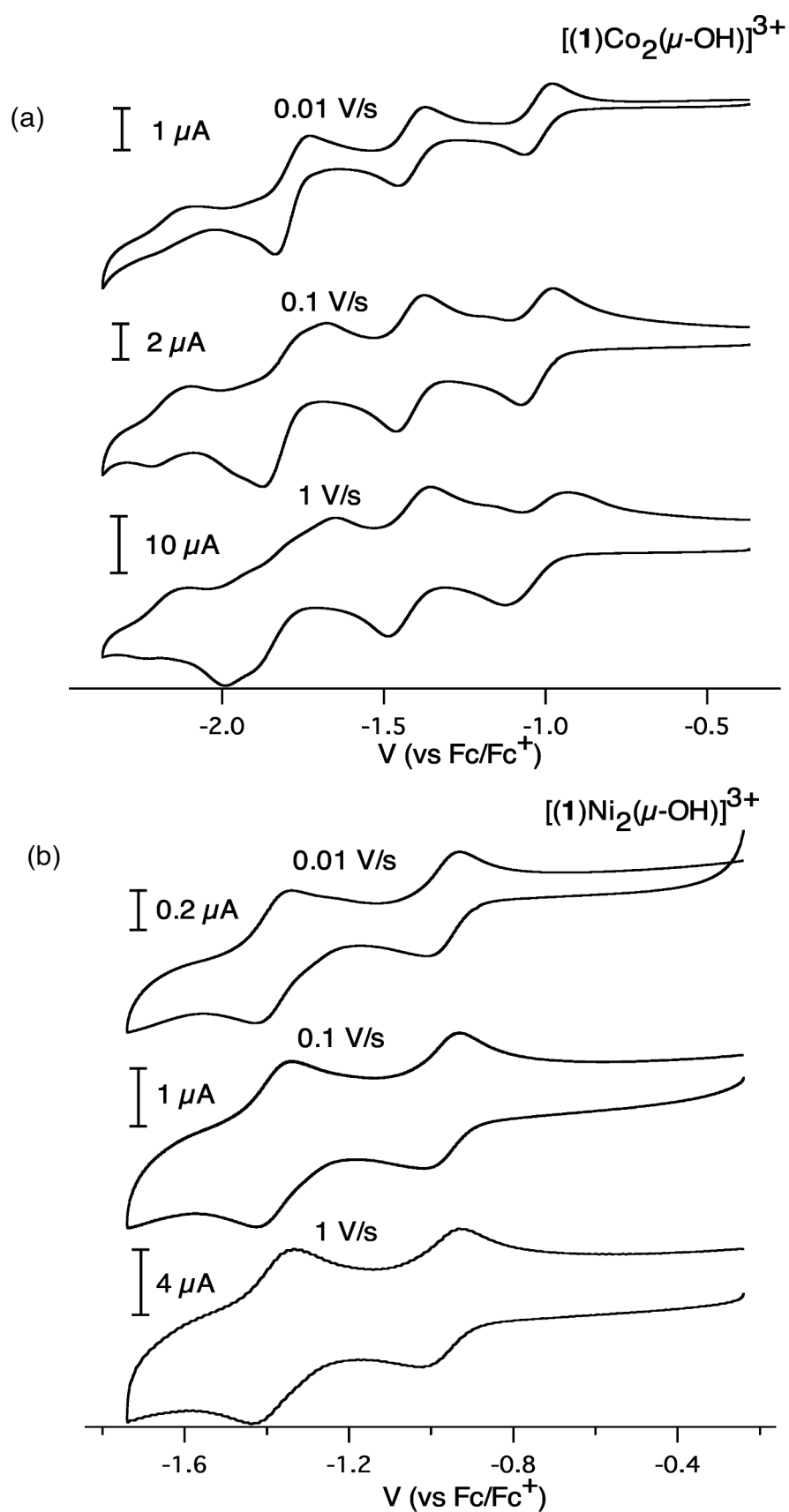


Figure S-5. Scan rate dependence of the cyclic voltammograms of (a)  $[(1)\text{Co}_2(\mu\text{-OH})]^{3+}$  and (b)  $[(1)\text{Ni}_2(\mu\text{-Cl})]^{3+}$ , in DMF with 0.1 M  $\text{Bu}_4\text{NPF}_6$ .



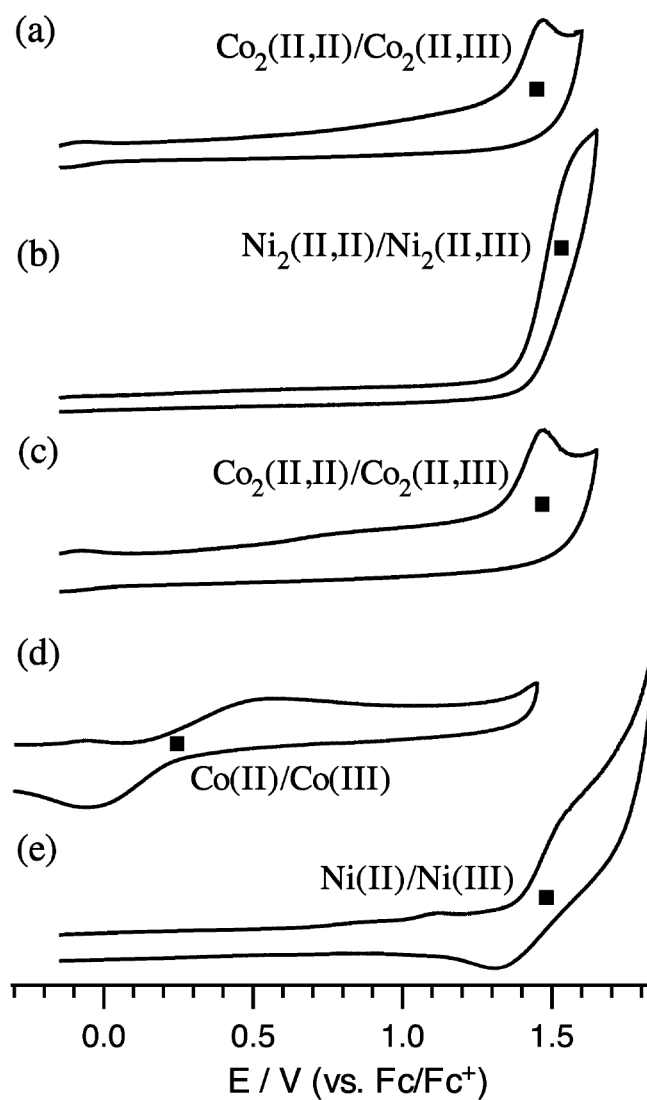


Figure S-6. Cyclic voltammograms (positive side) for (a)  $[(\mathbf{1})\text{Co}_2(\mu\text{-OH})]^{3+}$ , (c)  $[(\mathbf{1})\text{Ni}_2(\mu\text{-Cl})]^{3+}$ , (c)  $[(\mathbf{2})\text{Co}_2(\mu\text{-OH})]^{3+}$  (d) cobalt(II) mononuclear complex and (e) nickel(II) mononuclear complex in  $\text{CH}_3\text{CN}$  with 0.1 M  $\text{Bu}_4\text{NPF}_6$ .

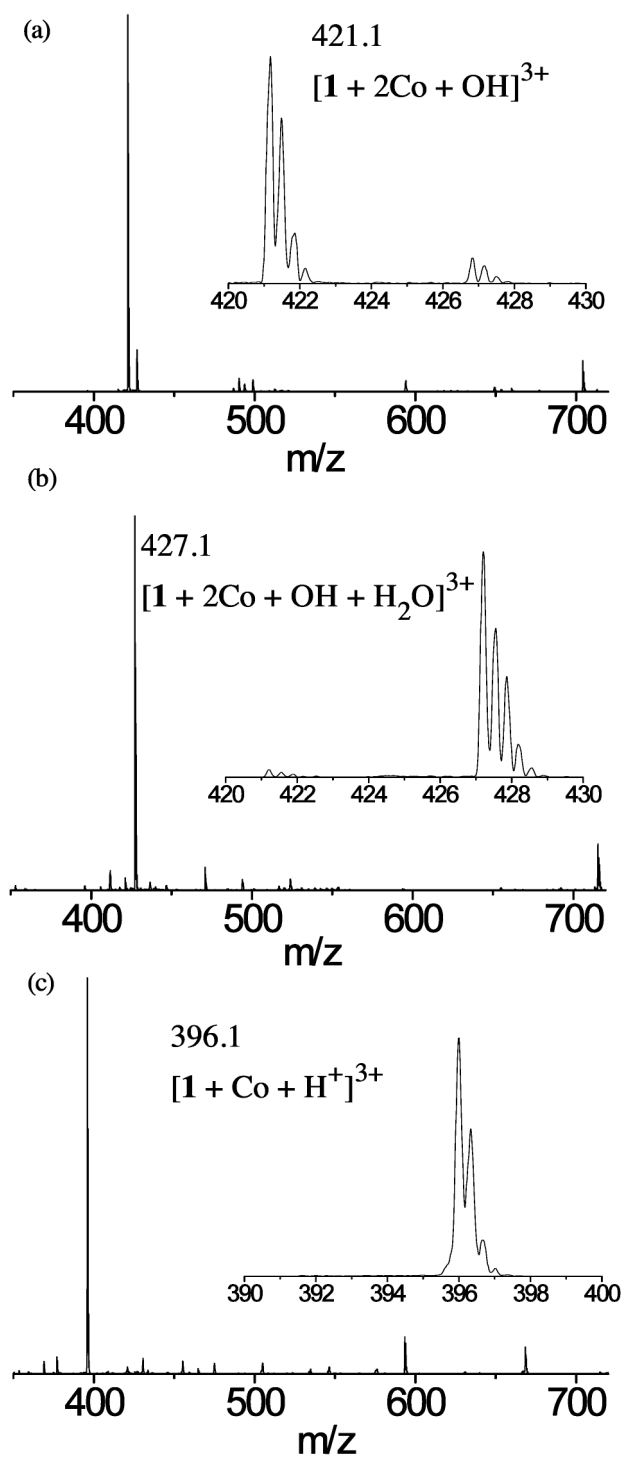


Figure S-7. ESI-MS spectra of (a)  $[(1)\text{Co}_2(\mu\text{-OH})]^{3+}$ , (b) after the addition of 10 eq.  $\text{CF}_3\text{SO}_3\text{H}$  and (c) after the addition of 30 eq.  $\text{CF}_3\text{SO}_3\text{H}$  in  $\text{CH}_3\text{CN}$ .

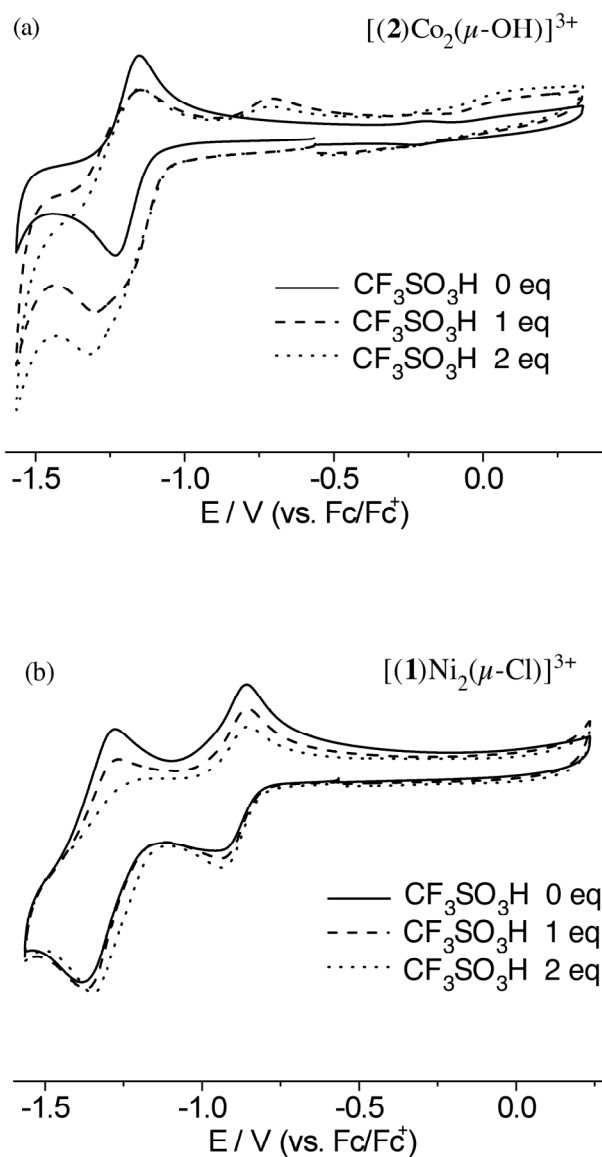


Figure S-8. CVs of (a)  $[(2)\text{Co}_2(\mu\text{-OH})]^{3+}$  and (b)  $[(1)\text{Ni}_2(\mu\text{-Cl})]^{3+}$ , with the addition of  $\text{CF}_3\text{SO}_3\text{H}$ .

Table S-1. Selected bond distances (Å) and angles (deg) for [(1)Ni<sub>2</sub>(μ-Cl)]<sup>3+</sup>.

Bond distances (Å)	
Ni-Cl	2.3699(6)
Ni-N1	2.107(2)
Ni-N2	1.992(2)
Ni-N3	2.124(2)
Ni-N4	2.093(2)
Ni-N5	2.090(2)
Bond angles (deg)	
Ni-Cl-Ni	104.40(3)
Cl-Ni-N1	93.30(5)
Cl-Ni-N2	91.43(5)
Cl-Ni-N3	90.78(5)
Cl-Ni-N4	92.42(5)
Cl-Ni-N5	168.57(5)
N1-Ni-N2	78.23(7)
N1-Ni-N3	156.23(7)
N1-Ni-N4	101.24(7)
N1-Ni-N5	95.04(7)
N2-Ni-N3	78.26(7)
N2-Ni-N4	176.13(7)
N2-Ni-N5	97.91(7)
N3-Ni-N4	101.97(7)
N3-Ni-N5	84.71(7)
N4-Ni-N5	78.30(7)